Monte Carlo Simulation of the Rod–Coil and Order–Disorder Transitions in Polynematic Macromolecules

Clive A. Croxton

Department of Mathematics, University of Newcastle, NSW 2308, Australia

Received December 14, 1989; Revised Manuscript Received June 25, 1990

ABSTRACT: Recent theoretical descriptions of the nematic order–disorder transition in polynematic macromolecules have generally concurred that there is a first-order transition between the disordered and aligned states of the system. The role of chain length and stiffness in determining the temperature at which the transition occurs is less conclusive, however. Here we present a Monte Carlo investigation of semiflexibly sequentially connected rods and determine the relationship between the order–disorder and the so-called rod–coil transitions. Particular attention is paid to the development of hairpins and their role in the rationalization of the behavior characteristics of the system.

Liquid-crystalline ordering in systems of semiflexible macromolecules has received considerable theoretical attention recently,[1-8] with particular attention being focused on the properties of the order–disorder transition and the rod–coil transition in such systems. It appears from some of these studies that these transitions are sensitive functions of the specification of the chain flexibility along the chain contour and the nature of the analytical approximations made in the course of its theoretical description. Given the somewhat idealized representation of the semiflexible macromolcule in the theoretical treatments, the most appropriate comparison with "experiment" is perhaps made in terms of a three-dimensional off-lattice Monte Carlo simulation where exactly the same parametric specification as for the theoretical calculations is used. We have previously reported the results of an iterative convolution (IC) description of semiflexible chain molecules,[4,7] and we now report the results of a Monte Carlo simulation of such a system providing a direct assessment of the IC analysis and a basis for comparison with other theoretical treatments. We observe from the outset that the qualitative agreement between the IC description and the current Monte Carlo estimates is excellent, and quantitative agreement between the IC and MC estimates is generally good.

The various theoretical analyses of the rod–coil transition in semiflexible linear sequences are generally made as a function of reduced temperature or chain concentration, and although these treatments differ as to how they model the chain flexibility (i.e., whether the flexibility is localized at the rod junctions or distributed homogeneously along its length), all treatments appear to confirm the existence of a transition from the coil to an extended or "rod" state with decreasing temperature or increasing concentration. Whether the order–disorder and rod–coil transitions are distinct and to what extent the stiffness and its distribution along the chain contour determine the nature of the transitions represent some of the primary objectives of this investigation, apart from providing a direct basis for the assessment of the iterative convolution estimates previously reported. Associated with this phenomenon there will, of course, be consequences for the mean square end-to-end length $\langle R_N^2 \rangle$ of the linear sequence of N rods and the mean square radius of gyration $\langle S_N^2 \rangle$. Monte Carlo simulations of such systems have been reported by Bluestone and Vold,[10] de Vos and Bellemans,[11] Baumgartner and Yoon,[12] and Khalatur et al.[13] invariably on the basis of chain concentration, which is only indirectly related to the present parametric description. Relatively little attention has been given to the Monte Carlo estimates of $\langle R_N^2 \rangle$, $\langle S_N^2 \rangle$, the orientational distribution functions, the development of hairpins, and length and flexibility dependence, all of which are important aspects of the rod–coil transition and of considerable theoretical and experimental interest: the study of these aspects represents one of the principal motivations for the current investigation. de Gennes[15] has implicated the role of hairpins in the rod–coil transition, and accordingly in this study we shall make a detailed investigation of their contribution to the geometrical properties of the system and their role in the reconciliation of a variety of transition phenomena that otherwise appear superficially inconsistent. Although not directly related to the present Monte Carlo investigations, a useful review of the lattice-based treatments of polynematic macromolecules has been presented by Flory.[5]

The IC technique, based on a statistical mechanical description of self-interacting polymer systems, has already been extensively described,[9] and its reiteration here is inappropriate. Suffice it to say, however, that in all previous IC analyses of self-interacting polymer systems comparison was invariably made with the results of a parametrically identical Monte Carlo simulation, and it is on this basis that we assert that the IC technique appears to provide a unified and highly successful description of polymer configuration. Khalatur et al.[13] have recently reported the results of Monte Carlo simulation in the vicinity of the nematic–isotropic transition as a function of concentration, and we shall refer to their work below.

In the present three-dimensional continuum Monte Carlo analysis we model the sequence on the same parametric basis as for our earlier iterative convolution (IC) description.[7] That is, the chain is considered to consist of sequentially connected unit rods, each of which experiences an orientational potential with respect to an external director field, and an *athermal* bend potential developed at the junction between sequentially adjacent rods. This choice of bend potential introduces a considerable simplification in the parametric description of the system in that we work in terms of reduced energy parameters, whereupon only the nematic and not the bend energy varies with temperature. Without this simplification in the description many features of the transition would be substantially obscured and make a direct comparison with the previously reported IC calculations impossible. Here, then, we adopt a cyclindrically symmetric "rectangular" bend potential, in which adjacent rods are flexibly connected but have a restricted relative

0024-9297/91/2224-0537$02.50/0

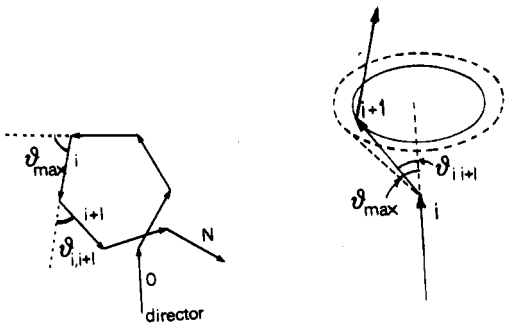

Figure 1. Geometry of polynematic sequence.

angular range θ_{max}:

$$\Phi(\theta_{i,i\pm1}) = 0 \quad \theta_{i,i\pm1} < \theta_{max}$$
$$= +\infty \quad \theta_{i,i\pm1} \geq \theta_{max}, 1 \leq i \leq N-1 \qquad (1)$$

Thus, for a perfectly rigid rod $\theta_{max} = 0$, while for a perfectly flexible chain $\theta_{max} = \pi$ (Figure 1). It is important to recognize that for this specification of chain flexibility the bend energy of the system is zero for all configurations satisfying the $\theta < \theta_{max}$ criterion. This choice of bend potential provides a useful means of assessment of the relative contributions of bend, flexibility, and orientational effects; the "rectangular" potential was also used throughout the theoretical IC calculations.

As many investigators have observed,[5,14,16] both steric and dispersion forces contribute to the stability of the nematic phase, and both types of interaction have featured in simulations and theoretical analyses of mesogenic systems. Steric effects are generally discussed in terms of athermal hard-rod or hard-ellipsoid representations in which concentration is the crucial parameter. "Soft" interaction theories, such as the Maier–Saupe treatment, are based upon mean field interactions arising from the dipole–dipole part of the anisotropic dispersion forces. In this kind of treatment the orientational potential of the ith rod in the mean field of its neighbors is of the form

$$\Phi(\theta_{0i}) = -\frac{AS}{V^m}(3\cos^2\theta_{0i} - 1)/2 \quad 1 \leq i \leq N \qquad (2)$$

where V is the molar volume. The ith rod is regarded as having an orientation θ_{0i} with respect to an external director field designated "unit vector 0" aligned along the z axis.

A, which varies from substance to substance, is a measure of the quadrupolar mean field and is taken to be independent of pressure, volume, and temperature, while m is generally taken to be 2, although Cotter has reviewed the postulates underlying the mean field approximation in the light of Widom's analysis and has concluded that thermodynamic consistency requires that $m = 1$, regardless of the nature of the intermolecular pair potential.[16] In our treatment we shall work in terms of the reduced potential

$$\Phi(\theta_{0i}) = -A^*S(3\cos^2\theta_{0i} - 1)/2 \quad 1 \leq i \leq N$$

where $A^* = A/k_BTV^2$, and shall neglect excluded-volume processes. This is not expected to substantially modify the conclusions drawn regarding the orientational features of the system. In what follows we may either regard the system as isothermal, whereupon A^* reflects the concentration of the system, or, conversely, regard A^* as a reduced reciprocal temperature at constant volume. Since the volume change at the transition is known not be large,[16] we shall generally regard A^* as a measure of reciprocal temperature. S is the nematic order parameter determined with respect to the external director and is defined in terms of the arithmetic mean over the chain segments:

$$S = \frac{1}{N}\sum_{i=1}^{N}\langle S_i\rangle \qquad (3)$$

where the "instantaneous" order parameter of the ith rod in a given chain configuration is

$$S_i = (3\cos^2\theta_{0i} - 1)/2$$

and $\langle S_i\rangle$ is the mean order parameter of the ith rod.

It is particularly important to distinguish between the "external" order parameter considered here and the "internal" order parameter of the rods defined with respect to the principal molecular axis of the molecule. For a relatively stiff chain the latter order parameter may remain high even at the lowest values of A^* (high temperatures), while the "external" order parameter may assume much lower values reflecting the orientational isotropy of the molecule. Careful attention should be paid in comparing our results with other analyses in which the distinctions between director, molecular axis, and chain backbone are less precisely drawn with some inevitable confusion in the resulting conclusions.[6,15] It follows that if we do not distinguish between parallel and antiparallel alignment along the director, then S varies between +1 and $-1/2$, corresponding to perfect alignment along and perpendicular to the director, respectively, while for a random distribution of the rods with respect to the director, $S = 0$.

Simulation of semiflexible chains of the kind described above presents an additional difficulty to those usually encountered in Monte Carlo simulation, and this arises from the fact that the chain–director interaction (eq 2) is a function of the (unknown) order parameter S. Clearly, the order parameter must be determined self-consistently with the interaction function eq 2, and this is achieved as follows. An initial estimate for the value of the order parameter, say S_0, is chosen. To expedite convergence, we generally take $S_0 = 0$ for $A^* < 4.5$ and $S_0 = 1$ for $A^* > 4.5$. This particular choice is made on the basis of the known Maier–Saupe result for isolated single rods and the iterative convolution results,[14,16] previously reported. We place the ith rod (i.e., choose $\theta_{i-1,i}$ and $\phi_{i-1,i}$) according to the probability density function $\exp(-A^*S_0(3\cos^2\theta_{0i} - 1)/2)$ within the range allowed by the bend potential and then treat all configurations as equally weighted. The energy of the system is determined on the basis of a look-up table with a step width of $\pi/32$ in $\phi_{i-1,i}$ and $1/32$ in $\cos\phi_{i-1,i}$ and $\cos\phi_{0,i-1}$. The usual Metropolis sampling technique is then followed, permitting a first estimate of the mean order parameter for the chain, say S_1 (eq 3), over a batch of configurations.

Batch means are treated as single measurements and accumulated until the confidence interval for S_1 is less than a predetermined limit; then the new value S_1 is compared with the original estimate, S_0. If the two values are consistent (our critrion is that they do not differ by more than 0.005), we begin to accumulate statistics for chains using the equilibrated S_1; if not, we substitute the new value, S_1, as our working estimate and repeat the process producing a further refinement, S_2, and so on. For the first estimate S_1 the limit on the confidence interval is fairly large (generally 5 times the final difference allowed between input and output S) to allow faster movement toward a more closely equilibrated value of S. As the value of S equilibrates, the limit on the confidence intervals is adjusted downward, ending at half the difference allowed between input and output S, or 0.0025.

We point out that we use *batch* means rather than individual configuration values for determining confidence intervals throughout the programs because the theoretical basis for the estimate of confidence intervals presumes that the data are measurements normally distributed about a true mean value.[17,18] The various quantities we measure may or may not satisfy this condition if individual configuration values are used. There is an optimum batch size, however, depending upon the length of the chains. If the batch sizes are too small, they may not yield a normal distribution of means, while if they are too large (for a given investment of computer time), the statistical data base may become inadequate. We found that up to 900 configurations per batch were necessary to achieve a normal distribution of means.

Once the equilibrated value of S has been determined, it may be used in eq 2 and the statistics allowed to accrue in the course of estimation of the configurational properties of the system. Thus, the mean square length of the chain containing rods p through q is

$$\langle R_{pq}^2 \rangle = \left\langle \frac{\exp(-\sum_i \Phi_{0i}) R_{pq}^2}{\exp(-\sum_i \Phi_{0i})} \right\rangle \tag{4}$$

and the mean square radius of gyration

$$\langle S_N^2 \rangle = \frac{1}{(N+1)^2} \sum_{p \geq q} \langle R_{pq}^2 \rangle \tag{5}$$

is also determined on the basis of the batched statistics described above, the simulations continuing until the errors are <2% for the longest chains investigated (N = 100).

Hairpin reversals along the director are identified by the product $\cos\theta_{0i} \cos\theta_{0,i+1} < 0$. Note that this criterion does *not* necessarily require a sharp reversal of the chain backbone: even for stiff chains in which chain reversals along the director are necessarily spatially extended structures, there must arise at some point along the contour the condition $\cos\theta_{0i} \cos\theta_{0,i+1} < 0$. By averaging over the batches of configurations, we are able to determine the average number of hairpins $\langle n_H \rangle$ as a function of chain length, stiffness, and reciprocal temperature and to determine their role in the rod–coil and order–disorder transitions.

Results and Discussion

In Figure 2a we show the nematic order parameter S determined on the basis of the present Monte Carlo simulations relative to the external director field as a function of reduced reciprocal temperature A^* for N = 50. The curves show a weak length dependence, although they appear to have reached their asymptotic form already by $N \gtrsim 10$. A more striking feature is the dependence upon stiffness, with the location of the order–disorder transition shifting to higher A^* with increasing flexibility and actually showing a *reversal* in the location of A^*_{NI} for flexibilities in the range $3\pi/4 \leq \theta_{max} \leq \pi$. These conclusions were anticipated in a previous publication[7] in which the iterative convolution results were presented. For comparison we show the corresponding IC transition curves for N = 10 (Figure 2b), and the quantitative agreement with the MC data is seen to be good.

This reversal in A^*_{NI} with increasing flexibility in the range $3\pi/4 \leq \theta_{max} \leq \pi$ may be regarded as an effective *stiffening* of the sequence due to the development of configurations of the form shown in Figure 3a in which

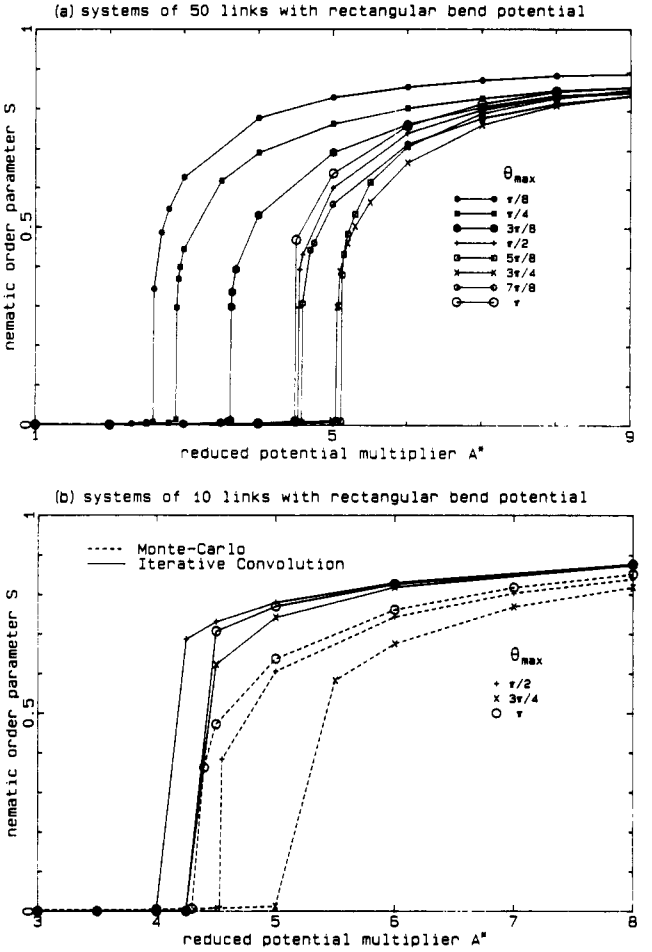

Figure 2. (a) Nematic order–disorder transition parameter S determined on the basis of Monte Carlo simulations as a function of reduced potential multiplier A^* for N = 50. Error bars cannot be resolved on this scale. (b) Order–disorder transition curves determined on the basis of the iterative convolution approximation.[7] Qualitative agreement with the Monte Carlo data is good. In particular note the reversal in the location of the transition with increasing flexibility (N = 10).

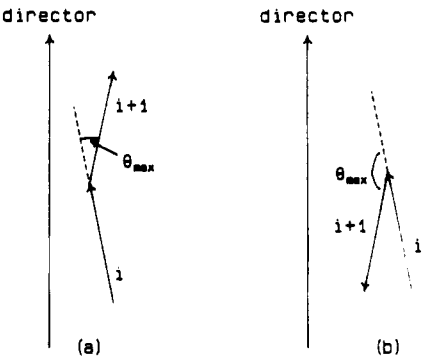

Figure 3. (a) Fully extended configuration of sequentially adjacent rods in an external director field. (b) Collapsed configuration. Both configurations are energetically identical for the present choice of rectangular bend potential (eq 1).

the rods attempt to comply with the strong external field. Of course, collapsed antiparallel configurations (Figure 3b) can always arise. However, the fully extended stiff configurations shown in Figure 3a can only arise for θ_{max} greater than some critical value, and this appears to be $\sim 3\pi/4$ on the basis of the Monte Carlo and iterative convolution determinations. It is appropriate to point out that for our choice of a "rectangular" bend potential configurations a and b are energetically identical, whereas

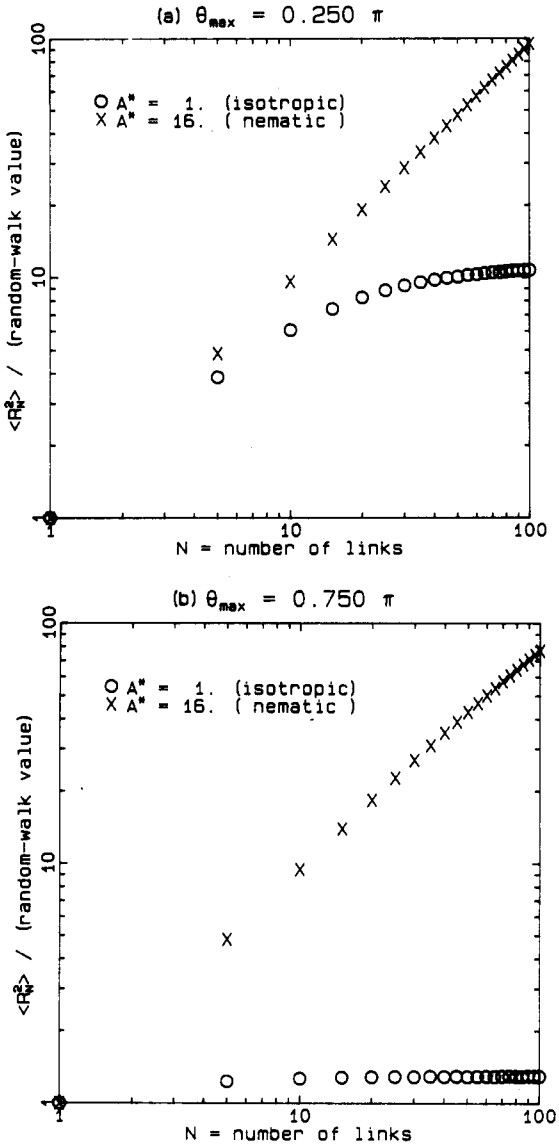

Figure 4. The ratio $\langle R_N^2 \rangle$/(random walk value) as a function of length for various stiffnesses at $A^* = 1$ and $A^* = 16$: (a) stiff chains ($\theta_{max} = 0.250\pi$); (b) flexible chains ($\theta_{max} = 0.750\pi$). The isotropic curves show a length-dependence characteristic at large N, while the nematic curves show a rodlike development with length.

for a harmonic bend potential, for example, $\Phi(i,i\pm1) = k^*(1 + \cos\theta_{i,i\pm1})^2$, between sequentially adjacent rods, low-stiffness, near-collinear configurations of the form a will be preferred to those of form b. The reversal in A^*_{NI} is almost certainly an idiosyncratic feature of our choice of bend potential as is the obvious departure from $A^*_{NI} \sim (\epsilon S)^{1/2}$ (ϵ = modulus of rigidity), which is thought to characterize the location of the transition.

Both the IC and MC estimates appear to confirm the development of a first-order transition in the order parameter curve, which, for perfectly flexible sequences, appears to coincide very closely with the Maier–Saupe result ($A^*_{NI} = 4.541$) for a perfectly stiff rod. Since in the case of perfect flexibility ($\theta_{max} = \pi$) the rods are effectively totally independent of one another, this result is not surprising; indeed, this result provides a useful check on the accuracy of the numerical procedures adopted in this analysis. Finally, to anticipate some of the later discussion, we draw the reader's attention to the fact that *all* chains, regardless of length or stiffness, exhibit a pronounced first-order transition between the ordered and disordered orientational states of alignment. We emphasize these features of the system prior to our discussion of the so-called "rod–coil" transition, which we shall attempt to distinguish from the order–disorder transition.

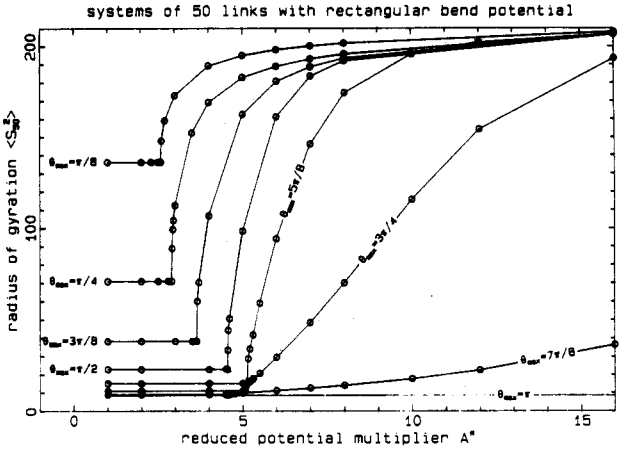

Figure 5. Mean square radius of gyration $\langle S_N^2 \rangle$ for chains of length $N = 50$ as a function of reduced potential multiplier A^* for various stiffnesses ($0.125\pi \leq \theta_{max} \leq \pi$). Error bars cannot be resolved on this scale.

The mean square end-to-end length $\langle R_N^2 \rangle$ and the mean square radius of gyration $\langle S_N^2 \rangle$ both show a highly sensitive dependence upon length and stiffness of the sequence (Figures 5 and 6). For comparison the corresponding estimates based upon the iterative convolution calculations are shown, and the qualitative agreement between the MC and the IC determinations is seen to be reasonably good (Figure 6b). The curves exhibit a number of striking features, in particular the extended thermal range over which coil elongation occurs, particularly for highly flexible systems. Indeed, for totally flexible sequences ($\theta_{max} = \pi$) the mean square length is *independent* of A^*, despite the pronounced transition in S: in no sense can a rod–coil transition be said to occur concurrently with that of the order–disorder parameter. The distinction between the two transitions is at its most marked for highly flexible sequences, although we observe that the *onset* of the elongation coincides with the A^*_{NI} of the S transition and even follows its reversal. Of course, for $A^* < A^*_{NI}$ we have $S = 0$, and the chain is decoupled from the external field. However, as soon as $S > 0$ coupling occurs and elongation commences. Although systems of low to intermediate flexibility appear to attain a rodlike state fairly rapidly, as evidenced by their close attainment of the asymptotic rod value of $\langle R_{50}^2 \rangle = 2500$, more flexible systems grow very slowly with increasing A^*—a result that we attribute to the entrapment of hairpins and the difficulty of their thermal elimination. This aspect will be discussed in more detail below. We do not agree that the rod–coil and order–disorder transitions can be separated simply by making the chains long enough as suggested by Wang and Warner[6] in the context of the worm model. The apparently contradictory behavior in S and $\langle R_N^2 \rangle$, particularly for systems of high flexibility, can be reconciled simply by recognizing that S has a quadrupolar dependence upon the external field (both parallel and antiparallel orientations yield high S) while $\langle R_N^2 \rangle$ has an essentially dipolar dependence whereby elongation is associated only with parallel alignments. A discussion in terms of the entrapment of hairpins will be given below.

The mean square radius of gyration $\langle S_{50}^2 \rangle$ for chains of length $N = 50$ determined on the basis of the present Monte Carlo calculations is shown in Figure 5. $\langle S_{50}^2 \rangle$ shows essentially the same behavior as $\langle R_{50}^2 \rangle$, as we might

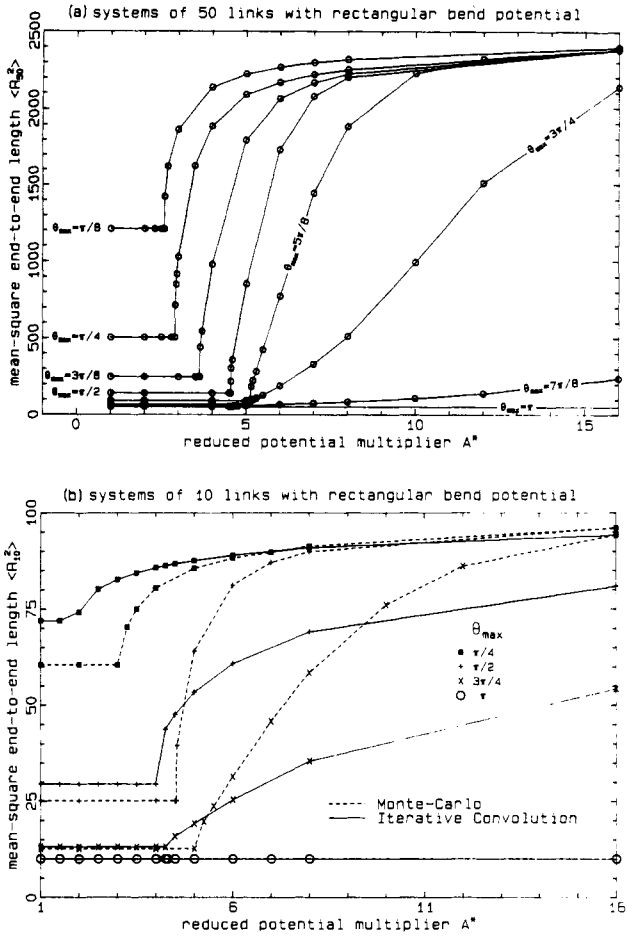

Figure 6. (a) Mean square end-to-end length $\langle R_N^2 \rangle$ for chains of length $N = 50$ as a function of reduced potential multiplier A^* for various stiffnesses ($0.125\pi \leq \theta_{max} \leq \pi$). (b) Mean square end-to-end length for chains of length $N = 10$ as a function of flexibility determined on the basis of the iterative convolution approximation.[7] The qualitative agreement with the Monte Carlo results is seen to be good.

anticipate, and a comparison with the IC estimates again confirms a good qualitative agreement between the theoretical and simulation descriptions. Both approaches indicate an extended elongation of the sequence with increasing A^* to an extent that depends upon chain stiffness, which, as we shall see below, may be related to the rate of thermal elimination of hairpins.

Given that the mean square length for perfectly flexible (random walk) systems $\langle R_N^2 \rangle_0$ shows no variation with A^*, the ratio $\langle R_N^2 \rangle / \langle R_N^2 \rangle_0$ is of interest, and we show this quantity as a function of chain length for two stiffnesses in the isotropic ($A^* = 1$) and the nematic ($A^* = 16$) phases (Figure 4). We see that in the isotropic phase the chains assume a random-walklike dependence (i.e., N^1) upon chain length at a rate depending upon the flexibility of the system. (Of course, the stiffer chains are expanded with respect to their perfectly flexible counterparts.) In the nematic phase the sequence shows a rodlike dependence (i.e., N^2) upon chain length and is only weakly sensitive to chain stiffness. The separation of the two curves of given flexibility represents (elongation)/N of the chain between the isotropic and nematic phases and grows steadily as expected. Stiffer systems show less relative elongation across the transition than do more flexible sequences (Figure 4a). Similar conclusions hold for the radius of gyration data.

These results appear to suggest that in the isotropic phase for sufficiently long systems the sequence ultimately

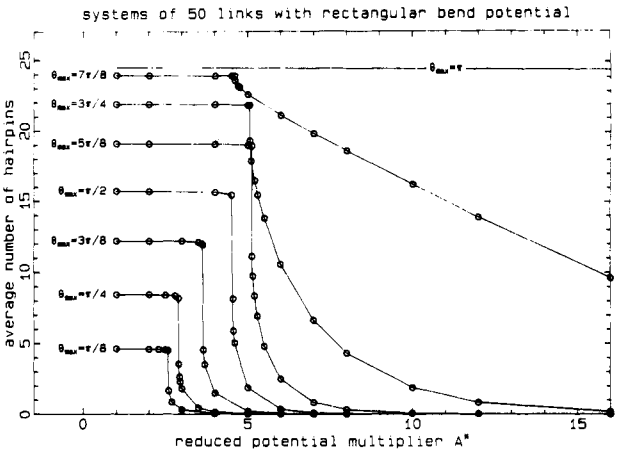

Figure 7. Number of hairpins $\langle n_H \rangle$ vs A^* for chains of length $N = 50$ of various stiffnesses. Error bars cannot be resolved on this scale.

achieves a random-walklike dependence upon N, while for the range of chain lengths investigated here, in the nematic phase the behavior is decidedly rodlike, even for highly flexible systems. The question then arises, how, in the nematic phase, with increasing flexibility is the random walk behavior regained? Even for a flexibility $\theta_{max} = 0.75\pi$ (Figure 4) there is only the slightest indication of a departure from rodlike behavior with N toward the isotropic value, yet we know that for total flexibility ($\theta_{max} = \pi$) $\langle R_N^2 \rangle$ regains random-walklike behavior in the nematic phase. Clearly, this aspect of the problem requires further resolution as to how this is brought about.

Hairpin reversals with respect to the director field are identified as $\cos \theta_{0i} \cos \theta_{0,i+1} < 0$ at one or more points along the chain contour. Even for relatively stiff chains in which hairpins are necessarily spatially extended features of the sequence there will nevertheless be an adjacent pair of rods for which the cosine product will be less than zero. Generally, the energy of the hairpin E_H will comprise a bend component E_B and a nematic component E_S arising from the traversal of the director field:

$$E_H = E_B + E_S$$

Hairpins are high-energy occlusions within the system and may be expected to exhibit an Arrhenius type of behavior. Indeed, de Gennes[15] discusses the probability of their formation in terms of a Boltzmann factor

$$\langle n_H \rangle \sim C \exp(-A^* E_H) \tag{6}$$

where $\langle n_N \rangle$ represents the number of hairpins and C is a constant of proportionality within a chain of given length and stiffness. For the present system $E_B = 0$ for configurations satisfying the rectangular bend potential condition $\theta_{i,i\pm1} < \theta_{max}$ (eq 1) and $E_S = 0$ for $A^* < A^*_{NI}$ (eq 2). For $A^* > A^*_{NI}$, however, $E_S > 0$, and for highly flexible systems in which E_S is likely to be small we may write

$$\langle n_H \rangle \sim C\left(1 - A^* E_S + \frac{(A^* E_S)^2}{2!} - \ldots\right) \tag{7}$$

For perfectly flexible sequences $E_S = 0$ in both the isotropic and nematic phases with the result that $\langle n_H \rangle = (N-1)/2$ for all A^*, a result clearly confirmed by the simulations for $N = 50$ (Figure 7). With decreasing flexibility we see that while E_S remains small, a linear representation (eq 7) describes the thermal elimination of hairpins, while as E_S increases, the exponential decay of $\langle n_H \rangle$ becomes apparent. Clearly, for highly flexible systems the hairpins

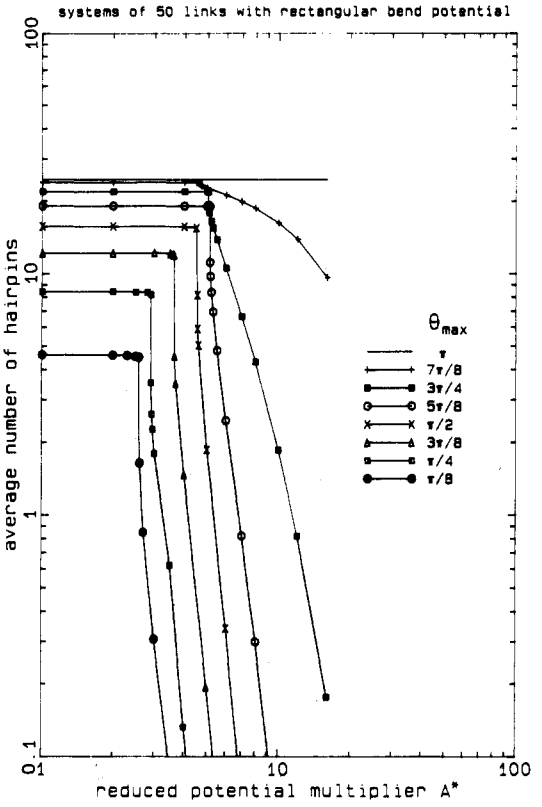

Figure 8. log $\langle n_H \rangle$ vs A^* for linear sequences of $N = 50$ links for various stiffnesses. The slopes represent the total hairpin energy E_H for the sequence, which is seen to decrease markedly with increasing flexibility.

become "frozen in": the activation energy associated with the cooperative traversal of the nematic field by large sections of the macromolecule which is required to release the hairpin ensures that their thermal elimination from the system is slow and occurs only over an extended thermal range of A^*. Precisely the converse is true for stiffer systems in which the development of spatially extended hairpins in the isotropic phase is relatively unlikely, and their elimination correspondingly rapid. It is clear that there is a close relationship between the thermal behavior of $\langle n_H \rangle$ and $\langle R_N^2 \rangle$ (and $\langle S_N^2 \rangle$) for a chain of given length and stiffness. All three quantities show the reversal in the location of the onset of the transition as the nematic potential discontinuously switches on with S at A^*_{NI}. However, $\langle n_H \rangle$, $\langle R_N^2 \rangle$, and $\langle S_N^2 \rangle$ all show a thermally extended development, depending upon stiffness, unlike the discontinuous variation of the order parameter. Clearly, the dipolar dependence of $\langle R_N^2 \rangle$ and $\langle S_N^2 \rangle$ upon the thermal elimination of hairpins proceeds slowly regardless of the high degree of quadrupolar alignment that characterizes the development of the order parameter S.

The qualitative form of the $\langle n_H \rangle$ vs A^* curves for various stiffnesses differs very little with increasing N, the differences being fully embodied in the prefactor C of eqs 6 and 7. A log–log plot of $\langle n_H \rangle$ vs A^* for $N = 50$ is shown in Figure 8, in which the slopes represent the total hairpin energy E_H of the sequence. Clearly, E_H decreases markedly with increasing flexibility, making their thermal elimination more difficult as described above.

Acknowledgment. I thank Ruby Turner for executing the numeral computations and the Australian Research Committee for financial support.

References and Notes

(1) Jähnig, F. *J. Chem. Phys.* **1979**, *70*, 3279.
(2) ten Bosch, A.; Maissa, P.; Sixon, P. *J. Phys., Lett.* **1983**, *44*, L105.
(3) Warner, M.; Gunn, J. M. F.; Baumgartner, A. B. *J. Phys. A: Math. Gen.* **1985**, *18*, 3007.
(4) Croxton, C. A. *Polym. Commun.* **1990**, *31*, 45.
(5) Flory, P. *Adv. Polym. Sci.* **1984**, *59*, 1.
(6) Wang, X.-J.; Warner, M. *J. Phys. A: Math. Gen.* **1986**, *19*, 2215.
(7) Croxton, C. A. *Macromolecules*, in press.
(8) Vroege, G. J.; Odijk, T. *Macromolecules* **1988**, *21*, 2848.
(9) Croxton, C. A. *J. Phys. A: Math. Gen.* **1984**, *17*, 2129.
(10) Bluestone, S.; Vold, M. J. *J. Chem. Phys.* **1965**, *42*, 4175.
(11) de Vos, E.; Bellemans A. *Macromolecules* **1974**, *7*, 809.
(12) Baumgartner, A.; Yoon, D. Y. *J. Chem. Phys.* **1983**, *79*, 521.
(13) Khalatur, P. G.; Papulov, Yu, G.; Pletneva, S. G. *Mol. Cryst. Liq. Cryst.* **1985**, *130*, 195.
(14) Maier, W.; Saupe, A. *Z. Naturforsch.* **1958**, *13a*, 564; **1959**, *14a*, 882; **1960**, *15a*, 287.
(15) de Gennes, P.-G. In *Polymer Liquid Crystals*; Ciferri, A., Krigbaum, W. R., Meyer, R. B., Eds.; Academic: New York, 1982; Chapter 5.
(16) Chandrasekhar, S. *Liquid Crystals*, Cambridge University Press: Cambridge, 1980; p 46 et seq.
(17) Bevington, P. R. *Data Reduction and Error Analysis for the Physical Sciences*; McGraw-Hill: New York, 1969.
(18) Bishop, M.; Frinks, S. *J. Chem. Phys.* **1987**, *87*, 3675.